JOURNAL OF COMPUTATIONAL
AND THEORETICAL NANOSCIENCE
Vol. 1. 81–87, 2004

A Nanoscale Spring-Loaded Valve Actuated by Colloidal Forces

Jonathan Fuchser, Prodip K. Das, Walied Moussa, and Subir Bhattacharjee*

Department of Mechanical Engineering, 4-9 Mechanical Engineering Building,
University of Alberta, Edmonton, AB, T6G 2G8, Canada

A spring-loaded valve analogue based on utilization of colloidal forces between two nano-particles in a confined domain is proposed. The governing principle of the proposed valve is that altering the surface potential of the walls of a confining cylindrical capillary can modulate the electrostatic component of the total colloidal force between two particles. This colloidal force can function as a restoring force of a spring-loaded valve acting against the external forces exerted by the fluid. Dynamic simulations of the valve actuation are presented, showing the motion of the microvalve components under the influence of different wall surface potentials and external forces. The simulations indicate that colloidal forces can be utilized effectively to actuate the valve under typical external loadings anticipated in microscale fluidic channels.

Keywords: Microfluidics; Spring-Loaded Valve; Colloidal Forces; Electrostatic Actuation; Finite Element Analysis.

RESEARCH ARTICLE

1. INTRODUCTION

Development of microvalves and pumps for controlled delivery of small volumes (μl to nl) of fluids has received significant attention over the recent years, specifically for rapid chemical analysis and detection using microfluidic chips for drug-delivery applications or delivery of coolants in microchips.[1–3] From amongst the different actuation mechanisms, electrostatic actuation tends to be the simplest from the viewpoints of implementation and operation.[3] Traditional designs of microvalves or micropumps employing electrostatic actuation resort to using a diaphragm or a cantilever that is subject to repeated cycles of stretching or bending stresses.[3–5] Such processes may limit the life of such components in a microdevice.

A large number of microfluidic applications involve dielectric fluids, which contain dissolved ions. If colloidal particles (small particles <5 μm in diameter) are suspended in a small volume of such a fluid, these particles can acquire a surface charge, the magnitude of which depends on the surface properties of the particles.[6, 7] Two similarly charged particles suspended in an ionic dielectric generally repel each other. Considerable attention has been devoted toward modeling, characterizing and measuring the nature of these electrostatic forces under a wide range of physico-chemical conditions.[8, 9] It has also been shown that confining these particles in a small domain with charged boundaries, for instance, between two parallel electrodes or in a narrow capillary enclosure, can substantially modify the interaction forces between them.[10–12]

The primary objective of this study is to modulate the colloidal force between two particles by altering the charges or potentials on the wall of the confining domain, thereby inducing a linear motion between the particles. The repulsion between the colloidal particles in the enclosure can be treated as a spring mechanism, counterbalancing an external force applied on one of the particles. Such an assembly may function as a spring-loaded valve for controlling the flow of a liquid into microfluidic channels. An advantage of such a colloidal device over traditional designs involving cantilevers or diaphragms stems from the absence of stretching, bending or frictional forces that can lead to failure of the device. Furthermore, this type of an assembly employs the natural colloidal forces representative of the length scales in nanoscale fluid handling systems, and does not involve the large external actuation forces typically employed in microfluidic control devices involving piezoelectric or other types of modulation techniques.

*Author to whom correspondence should be addressed.

In this paper, we outline the mechanisms of force modulation between two spherical colloidal particles induced by the charged confining walls of a cylindrical capillary and qualitatively investigate how the force depends on the charging behavior of the confining domain boundary as well as some of the key physico-chemical conditions of the system. Based on these theoretical results, we suggest application of the system as an electrostatic actuator that can function as a spring-loaded microvalve. Numerical simulations of the system with different magnitudes of external loadings are then conducted to show the range of operating conditions over which such a valve mechanism can successfully operate.

2. MATHEMATICAL MODEL

2.1. Concept and Physical Description of a Colloidal Spring-loaded Valve

The colloidal microvalve concept is depicted in Figure 1, which shows the basic principle of a spring-loaded valve (Fig. 1a), followed by a conceptual diagram of a colloidal microvalve, where the colloidal interaction force between two particles acts as the spring (Fig. 1b). Both the figures depict a fixed colloidal particle located at the end of a cylindrical capillary, and a second colloidal particle, which can translate axially, depending on the various forces acting on it. In the case of a spring-loaded valve, Fig. 1a, the spring is compressed by an external force. Depending on the magnitude of the restoring force of the spring connecting the two particles relative to this external force, the location of the moving particle can be altered. As long as the external force is smaller than the restoring force of the spring, the two particles will be farthest apart (corresponding to the relaxed length of the spring). When the magnitude of the force is greater than the restoring force of the spring, the latter will be compressed, and the movable particle will be brought closer to the fixed particle. By carefully placing an outlet channel on the cylinder wall such that the relaxed and the compressed positions of the movable particle exist on two sides of the outlet, a spring-loaded microvalve can be conceived.

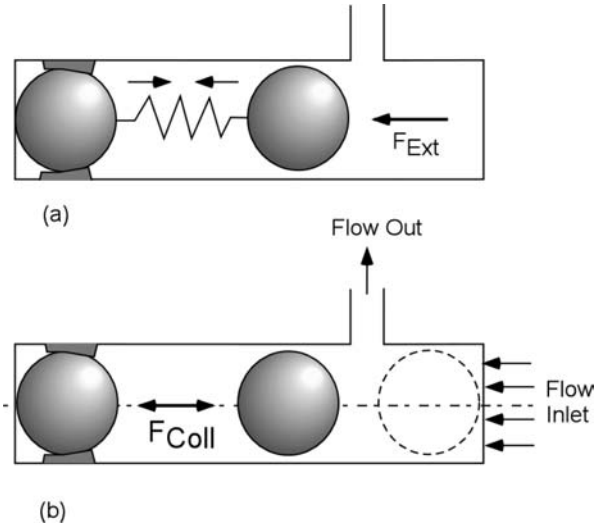

Figure 1. Concept diagram of a colloidal force actuated spring-loaded valve. The spring in part (a) is replaced by the colloidal repulsion in part (b).

The colloidal microvalve is envisioned to work in a similar manner. However, in this case, the restoring force of the spring is replaced by the restoring force due to the colloidal repulsion between two similarly charged particles. In addition to removal of a mechanical spring from between the particles, this arrangement will also allow the modulation of the restoring colloidal force by altering the surface potential on the confining cylindrical wall. Thus, even when the movable particle is subject to a fixed external force, modulation of the restoring colloidal force can open or close the valve. The fundamental question regarding the concept of such a valve is to what extent can the restoring colloidal force between the two particles be modulated and what will be the range of operation of such a valve? In the following, we develop the mathematical principles underlying such a device, which will be the basis for addressing this question.

2.2. Estimation of the Colloidal Forces

The overall interaction force experienced by the mobile colloidal particle will be a combination of an attractive van der Waals (VDW) interaction force and, for similarly charged particles, a repulsive electrostatic double layer (EDL) force. In the framework of the Derjaguin-Landau-Verwey-Overbeek (DLVO) theory,[13, 14] the total colloidal force between the two particles can be expressed as

$$F_{Coll} = F_{VDW} + F_{EDL} \tag{1}$$

For particles in a tightly fitting cylindrical enclosure, we need to evaluate the interaction force components by taking into account the close proximity of the cylindrical wall, its material and its interfacial properties.

2.2.1. van der Waals Force

The van der Waals interaction energy on a spherical particle enclosed in a cylindrical capillary was derived by Bhattacharjee and Sharma.[15] Based on this study, it becomes apparent that for an isolated spherical particle located at the centerline of a cylindrical capillary, there will be no net van der Waals force imposed on the particle due to the cylinder wall. Assuming a pairwise additivity of van der Waals forces (Hamaker's approach), the net van der Waals force experienced by the mobile particle will simply be the interaction force due to the fixed particle as long as the particles are confined to the centerline of the capillary. An analytic expression for the van der Waals interaction force based on Derjaguin's approximation technique is

$$F_{VDW} = -\frac{A_H a}{12h^2} \quad (2)$$

where A_H is the effective Hamaker constant for the system, a is the particle radius (assuming both particles are of same size) and h is the surface-to-surface separation distance between the two colloidal particles. It should be noted that the above expression for the van der Waals interaction force is based on Derjaguin's approximation, which leads to an overestimation of the force at large separations between the particles, particularly when $h \gg a$.[16] Furthermore, the above expression does not consider the effects of retardation, which diminishes the van der Waals forces as the separation between the particles increase. Equation (2), however, provides an upper bound of the van der Waals interaction possible for a given colloidal system by means of a simple expression.

2.2.2. Electrostatic Double Layer Force

The second component of the total colloidal force, namely, the electrostatic double layer interaction force, cannot be evaluated in terms of an analytic expression. In this case, a detailed solution of the governing electrostatic equation must be obtained for the given geometry. The governing equation for the EDL force is the Poisson-Boltzmann equation, which is solved numerically by employing the finite element technique. Figure 2 shows the cylindrical geometry under consideration in the present investigation along with the coordinate framework. Here, two spherical colloidal particles of radius a are separated by a distance h (distance of closest approach) in a cylindrical capillary of radius b. The interaction forces between the particles are determined at various separation distances, assuming that the particle centers always lie on the plane of axial symmetry. This allows the solution of the three-dimensional problem in an axisymmetric two-dimensional coordinate system. The ratio of the radius of the cylindrical capillary to the particle radius is denoted as the aspect ratio A ($= b/a$).

Utilizing the axisymmetry when the particles are axially located in the capillary, the governing Poisson-Boltzmann (PB) equation can be written in the cylindrical coordinate system as

$$\frac{\partial^2 \Psi}{\partial \bar{r}^2} + \frac{\partial^2 \Psi}{\partial \bar{z}^2} = \sinh(\Psi) - \frac{1}{\bar{r}} \frac{\partial \Psi}{\partial \bar{r}} \quad (3)$$

where Ψ ($= ve\psi/kT$) is the scaled potential, and the scaled coordinates are $\bar{r} = \kappa r$ and $\bar{r} = \kappa z$. The coordinates are scaled with respect to the Debye screening length κ^{-1}. For a symmetric (ν:ν) electrolyte, the screening length is

$$\kappa^{-1} = \sqrt{\frac{\varepsilon \varepsilon_0 kT}{2n_\infty e^2 \nu^2}} \quad (4)$$

where n_∞ is the bulk concentration of the ions (in numbers/m^3), ε is the dielectric constant of the suspending fluid, ε_0 is the dielectric permittivity of vacuum, e is the fundamental charge, ν is the valence of the ions, k is the Boltzmann constant and T is the absolute temperature. In the present investigation, we consider constant potential (CP) boundary conditions for the particle and capillary wall surfaces.

The boundary conditions for the problem are (Fig. 2):

$$\Psi = \Psi_p \text{ for } \partial\Omega \in \text{BCD and EFG} \quad (5a)$$

$$\Psi = \Psi_c \quad \text{for} \quad \partial\Omega \in \text{IJ} \quad (5b)$$

$$\mathbf{n} \cdot \nabla\Psi = 0 \text{ for } \partial\Omega \in \text{AB, DE, GH, HI, and JA} \quad (5c)$$

The last statement, Eq. (5c), where $\mathbf{n}$ represents the unit normal to the surface, provides the symmetry conditions on the fluid boundaries, implying that the potential gradients normal to these line segments are zero. Clearly, this is an artificial boundary condition on segments JA and HI, and these boundaries should be placed sufficiently far away from the particles to ensure that this artificial boundary condition does not influence the accuracy of the solution. To solve Eq. (3) numerically, we used the finite element technique with adaptive mesh refinement as described in our earlier work.[12] The finite element simulations were performed using FEMLAB® (COMSOL, Inc.) software running on a MATLab (Mathworks, Inc.) platform in a personal computer (with a 2.4 GHz Pentium IV processor and 2 GB of RAM).

Once the electric potential and field distributions are obtained by solving the PB equation, the net electrostatic force between the two particles is obtained by integrating the stress tensor on the closed surface of one of the particles. The stress tensor comprises an isotropic osmotic stress contribution and the Maxwell stresses arising from the electrostatic field. Combining these, the electrostatic force on the spherical colloidal particle is expressed as

$$\mathbf{F} = \iint_S \mathbf{T}_{ij} \cdot \mathbf{n} dS = \iint_S \left[\left(\Pi - \frac{1}{2} \varepsilon \varepsilon_0 \mathbf{E} \cdot \mathbf{E} \right) \mathbf{I} + \varepsilon \varepsilon_0 \mathbf{E}\mathbf{E} \right] \cdot \mathbf{n} dS \quad (6)$$

Here $\mathbf{F}$ is the force acting on the sphere, $\mathbf{T}_{ij}$ is the electrostatic stress tensor, $\mathbf{E}$ ($= -\nabla\psi$) is the electrostatic field vector, Π is the osmotic pressure difference between the electrolyte at the particle surface and the bulk electrolyte, $\mathbf{n}$ is the unit outward surface normal and $\mathbf{I}$ represents the identity tensor.

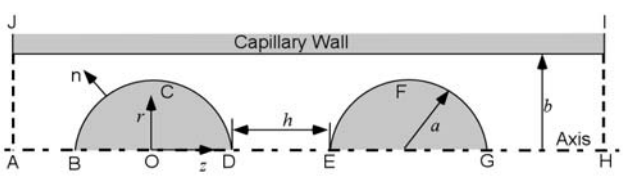

Figure 2. Schematic representation of the computational domain used for the calculation of the EDL force.

The net force acting on a sphere along the axial (z) direction can be determined from the component of Eq. (6) acting along the axial (z) direction. Utilizing the fact that the integral of the isotropic osmotic pressure term over a closed surface of constant potential is always zero, the force acting along the z direction can be written explicitly as

$$F_z = \mathbf{F}\cdot\mathbf{k} = 2\pi\kappa^2\varepsilon\varepsilon_0\left(\frac{kT}{ve}\right)^2 \int_{S_p}\left[n_r E_r E_z + \frac{1}{2}n_z\left(E_z^2 - E_r^2\right)\right] r\mathrm{d}r \tag{7}$$

where $\mathbf{k}$ is a unit vector in the positive z direction, n_r and n_z are the components of the unit surface normal vector $\mathbf{n}$ along the r and z directions, respectively, and S_p (the arc BCD in this present case) represents the semi-circular boundary of the spherical particle over which the integration is performed. E_r and E_z are the components of the electric field vector $\mathbf{E}$ along the r and z directions, respectively. Finally, the axial force is represented in its non-dimensional form, given by

$$f_z = \frac{F_z}{\varepsilon\varepsilon_0}\left(\frac{ve}{kT}\right)^2 \tag{8}$$

We note here that since the force is calculated on the sphere BCD with its center at the origin, a repulsive force on this sphere will be directed toward the negative z direction, while an attractive force will act along the positive z direction.

2.3. Calculation of the Particle Positions

Evaluation of the total colloidal force acting on the mobile particle provides the net restoring force for the spring-loaded valve system. We now turn our attention to the nature of the external force acting on the mobile particle. In most cases, it will be the force exerted by the fluid in the capillary pushing on the particle. In other words, we can consider it an arbitrary external force acting on the mobile particle due to the fluid pressure. When the total force, obtained by combining the colloidal and external forces, acts on the mobile particle, the particle will move under the influence of these forces until it reaches an equilibrium position where the colloidal force balances the external force. However, as soon as the particle moves relative to the liquid in the capillary, there will be a drag force acting on the particle opposing its motion. A simple approximation for the drag force will be the Stokes-Einstein drag force on a spherical particle exerted by a fluid for a given relative velocity between the particle and the fluid, expressed as

$$F_{drag} = 6\pi\mu a u \tag{9}$$

where μ is the liquid visocisty, a is the particle radius and u is the relative velocity of the particle with respect to the fluid. At equilibrium, the drag force will equal the total force. Equating the forces, we can obtain an expression for the particle velocity under the combined influence of colloidal, external and hydrodynamic forces by assuming a non-accelerating system. In other words, combining Eqs. (1) and (9), we obtain

$$u = \frac{F_{EDL} + F_{VDW} + F_{Ext}}{6\pi\mu a} \tag{10}$$

The above equation represents a simple trajectory equation for the mobile particle by noting that

$$\frac{dz}{dt} = u = \frac{F_{EDL} + F_{VDW} + F_{Ext}}{6\pi\mu a} \tag{11}$$

where the term dz/dt denotes the axial displacement of the mobile particle under the influence of all the forces.

2.4. Solution Methodology

The trajectory of the mobile particle was computed using a quasi-steady iterative solution of Eq. (11). The colloidal force on the mobile particle was varied by changing the surface potential on the cylindrical capillary wall. The simulations were started with a given initial separation, h_0, between the two particles. We assumed a sinusoidal variation of the cylinder wall surface potential given by

$$\Psi_c(t) = \Psi_{c,\max}\sin(\omega t) \tag{12}$$

where $\Psi_{c,\max}$ is the scaled amplitude of the surface potential and ω is the frequency with which the potential is oscillated over time. At a given instant, the wall potential determined using Eq. (12) was used in the finite element solution of the Poisson-Boltzmann Equation (3) to obtain the electrostatic force at that instant. The van der Waals interaction was computed using Eq. (2) for the given separation. Once these forces were obtained, the external force was added to the total colloidal force, Eq. (1), and the particle velocity was obtained using Eq. (11). Next, assuming that the particle translates under this steady velocity over the given time interval, we determine the displacement of the particle from the initial position. The procedure is then repeated over successive time steps.

One should note that this is an approximate procedure assuming that the steady-state colloidal forces are attained almost instantaneously compared to the overall dynamics of the particle motion. In other words, the electrostatic double layer interactions equilibrate at a time scale much smaller than the time scale of the hydrodynamic relaxation. This assumption is usually considered to be fairly accurate for most colloidal systems since the time scale for the relaxation of the ionic equilibrium is about three orders of magnitude smaller than the time scale of the hydrodynamic relaxation for a colloidal particle. Furthermore, if we carefully select the time steps for solving Eq. (11) to be

large enough to enable the electrostatic equilibrium to be established, and allow the surface potential on the wall to change slowly, the present solution technique will be a fair approximation of the particle dynamics in the given system.

3. RESULTS AND DISCUSSION

3.1. Effect on Electrostatic Forces from a Sinusoidal Variation of Wall Surface Potential

The influence of the time varying wall surface potential on the scaled electrostatic interaction force is depicted in Fig. 3. Here, the scaled force on a particle for a fixed scaled surface-to-surface separation, $\kappa h = 0.4$, is shown corresponding to the variation of the scaled cylinder wall surface potential Ψ_c ($= ve\psi_c/kT$) between $+3$ and -3 over a time interval of 10 seconds. The simulations were performed for a scaled particle radius, $\kappa a = 1$, and the aspect ratio $b/a = 1.2$. The scaled surface potential of the particles was $+3$. For these conditions, the simulation results indicate that, as the wall surface potential becomes equal to the particle surface potential, the interaction force approaches zero while the interaction force magnitude becomes maximum when the signs of the wall and particle surface potentials are opposite. We note that in Fig. 3, the negative value of the force corresponds to repulsion. Hence, the repulsion between the two particles can be modulated over a relatively large range by varying the cylinder surface potential by about 75 mV.

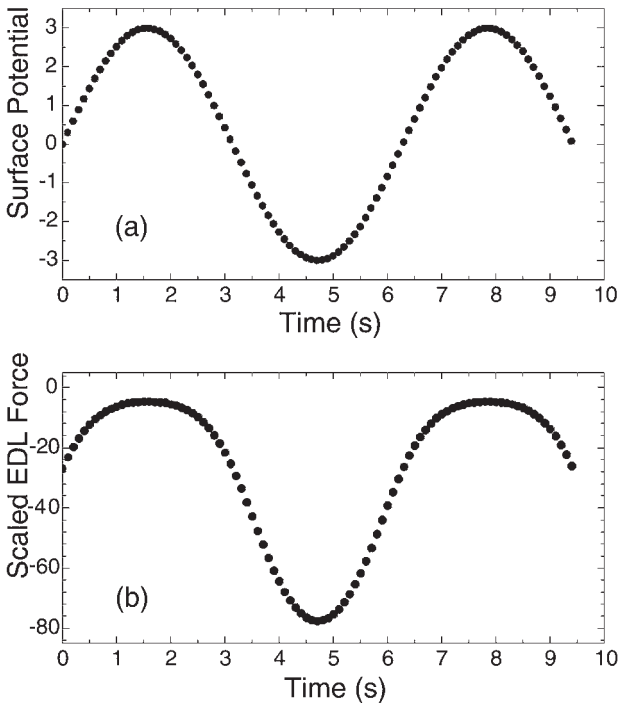

Figure 3. A layered plot of scaled surface potential over time in part (a) and scaled EDL force in part (b) when wall potential (Ψ_c) is cycled at a frequency of 10 rads/s between $+3.0$ and -3.0. The simulation was performed for a scaled particle separation (κh) of 0.4 and a scaled particle radius (κa) of 1.0.

This variation can be treated as a modulation of the spring constant of a spring-loaded valve. When the cylinder wall is given an opposite charge compared to the particle surface charge, the stiffness of the spring in enhanced, while the stiffness is reduced as the cylinder and the particle surface potentials become equal.

3.2. Effect of Particle Separation on DLVO Forces

Figure 4 depicts the variation of the DLVO force acting on the mobile particle with scaled separation distance for three representative values of the scaled wall surface potential amplitude ($\Psi_{c,max} = +3$, 0 and -3). The scaled particle surface potential was -3 for these simulations, while the scaled particle radius (κa) was 1. The van der Waals force was evaluated using a value of 1×10^{-20} J for the Hamaker constant. It is observed that the total DLVO interaction force shows a higher peak value when the cylinder and particle surface potentials are different, with the highest forces obtained for opposite signs and equal magnitudes of the surface potentials. When the cylinder and particle surface potentials are identical, the interaction force is very small. The DLVO force becomes attractive at very small separations.

If an external force is applied on the mobile particle opposing the DLVO repulsion, its magnitude will dictate the motion of the particle for different values of the wall surface potential. For instance, consider an external force of 2×10^{-11} N, as shown in Fig. 4. For this force, we note that if the wall and particle surface potentials are $+3$ and -3, respectively, then the equilibrium position of the mobile particle will be *ca.* $\kappa h = 0.725$, corresponding to the location when the total force is zero. However, when the wall sur-

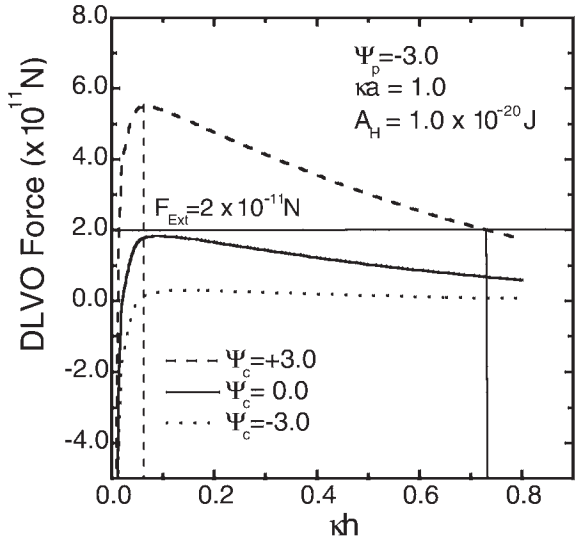

Figure 4. Variation of the DLVO force acting on the mobile particle with scaled separation distance between the particles (κh) corresponding to different cylinder surface potentials. The electrostatic force was calculated using a fixed surface potential ($\Psi_p = -3.0$) on the particles. The scaled particle radius (κa) was 1.0, while the van der Waals force was evaluated using a value of 1.0×10^{-20} J for the Hamaker constant.

RESEARCH ARTICLE

face potential is changed to zero, the external force will push the mobile particle until it comes in contact with the stationary particle. Thus, variation of the wall surface potential will alter the restoring colloidal force acting on the mobile particle, and the mobile particle can be made to move back and forth as the wall surface potential is switched on and off. It should be noted, however, that the particles cannot be allowed to touch each other since the force will become infinitely attractive at contact and it will be impossible to move the mobile particle away if it comes in contact with the stationary particle. Therefore, the closest distance to the stationary particle to which the mobile particle can approach should be limited. This location is shown using the dashed vertical line in Fig. 4. Typically, in the rest of the paper, we use a cut-off distance $\kappa h_{min} = 0.05$, which generally corresponds to the location of the repulsive peak of the DLVO force profiles.

The distance between the maximum equilibrium separation and the cut-off separation will represent the sweep of the mobile particle under the influence of a given external force. It is clear that reducing the magnitude of the external force will increase the sweep. Furthermore, continuously changing the cylinder surface potential in a periodic manner will result in a back-and-forth movement of the mobile particle between the two extreme positions for a given external force. Such a mechanism can be utilized as an automatic valve that can supply fluid at a specified rate determined by the speed at which the wall potential can be oscillated.

3.3. The Colloidal Microvalve

In this subsection, we present the simulation results based on the trajectory analysis for prediction of the motion of the mobile particle under the influence of the varying wall surface potential and the external force. Figure 5 depicts the movement of the mobile particle under an applied external force of 1.5×10^{-11} N for three different values of the wall surface potential amplitude ranging from 1 to 5. The simulations depict one full sweep of the valve under each set of conditions. The minimum separation between the mobile and stationary particle was fixed at 5 nm. The particle scaled surface potential was -3 for all the simulations. The total displacement of the mobile particle increases with an increase in the wall surface potential. For the wall surface potential of 1, the particle travels a distance of about 50 nm between the maximum and minimum displacements from the stationary particle. For the wall potential of 5, the total displacement of the particle increases to *ca*. 90 nm. The separation between the mobile and the stationary particles is maximum when the wall and particle surface potentials bear opposite signs.

As the wall potential is varied in a sinusoidal manner, the repulsive colloidal force decreases in magnitude. The magnitude of the force is minimum when the wall potential attains the same sign as the particle potential and has the

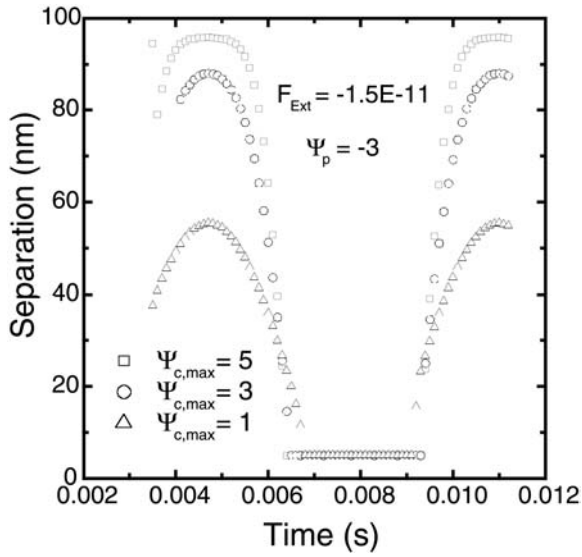

Figure 5. Actuation of mobile particle under a fixed external load when a sinusoidal surface potential is applied on the cylinder wall. The different symbols correspond to different surface potentials on the cylinder wall as indicated in the legend. The scaled particle surface potential was -3.0 for these simulations, while the scaled particle radius was 1.0.

highest value (the opposite crest of the sinusoidal variation). Under this condition, the external force pushes the mobile particle toward the stationary particle until the mobile particle is pushed to its minimum allowable separation from the stationary particle. As the wall surface potential is increased back to its other peak value, the mobile particle moves back to larger separations. The increase in the sweep with the increase in the amplitude of the wall surface potential is not linear. At wall potentials higher than the magnitude of the particle surface potential, the influence of the colloidal forces on the sweep of the valve is not as dramatic.

The variation of the sweep with the magnitude of the external force is depicted in Fig. 6. Here, the maximum distance over which the mobile particle can move, when corresponding to an applied external force, is shown for two values of the wall surface potential amplitude. The external force is plotted as a negative quantity since it acts opposite to the colloidal force. The particle surface potential was -3 in these simulations. It is evident that the sweep is diminished as the external force is increased. Furthermore, for a given external force, the sweep is lower when the wall surface potential amplitude is small. Combining the amplitude of the wall surface potential modulation and the magnitude of the external force, one can obtain enormous flexibility in determining the sweep of the colloidal spring-loaded valve.

The variation of the sweep with the wall surface potential amplitude is shown in Fig. 7 for three fixed values of the external force. For small external forces, we obtain a fairly large sweep at low amplitudes of the wall surface potential. As the external force becomes large, the sweep shows a non-linear variation with the amplitude of the wall surface potential. In fact, for wall surface potential amplitudes greater than 3, the sweep cannot be significantly increased.

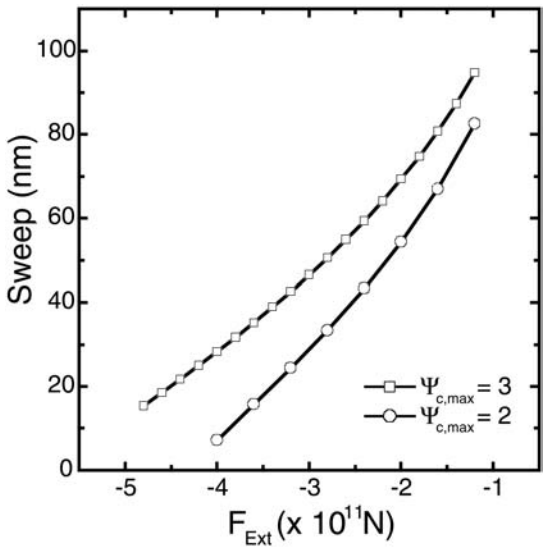

Figure 6. Range of colloidal actuation or sweep of mobile particle with fluid drag (F_{Ext}) for two different cylinder potentials as indicated in the legend. Other simulation parameters were identical to Fig. 4.

To summarize, the present simulations indicate that a nanoscale spring-loaded valve concept can be realized by utilizing the colloidal repulsion forces. The spring stiffness of such a valve can be modulated and precisely controlled by changing the capillary wall surface potential. Provided that the capillary wall surface potential can be varied with time, such a valve can act as an automatic sampling device for microfluidic systems. The simulations presented here, although performed under a quasi-steady assumption, should provide adequate insight regarding the dynamics of the valve. A more rigorous transient solution will be necessary if the wall surface potential is oscillated at substantially higher frequencies.

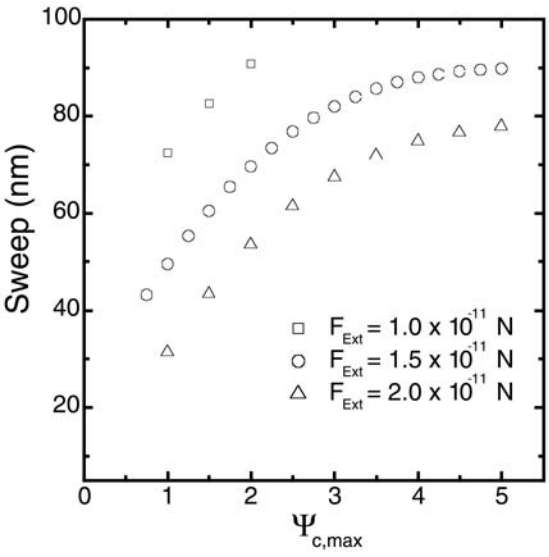

Figure 7. Range of colloidal actuation or sweep of mobile particle with wall surface potential amplitude for three fixed values of the external force under same conditions as Fig. 4.

4. CONCLUDING REMARKS

A colloidal microvalve based on the force modulation between two colloidal particles induced by the charged confining walls of a cylindrical capillary is proposed. The numerical simulation results reveal that the net DLVO force between the particles can be modulated over a wide range by applying different levels of surface potential on the cylinder wall. The influence of periodic surface potential of the cylinder wall on the interaction force is more pronounced when the cylinder wall is given an opposite potential (in sign) compared to the particles surface potential. Conversely, the interaction force is small for similarly charged capillary, and the DLVO force becomes attractive at very small separations. Under an external drag force of 15.0 pico-N, approximately 90 nm of sweep can be achieved by varying the cylinder surface potential by about 75 mV. However, higher surface potential on the cylinder wall does not show any significant variation of the sweep. Based on these results, it seems possible to utilize this force modulation between the colloidal particles to control the flow through a microchannel. It is also noted that the proposed microvalve can be easily implemented by trapping two colloidal particles in a cylindrical or rectangular channel using standard microfabrication techniques.

References

1. M. Gad-el-Hak, *The MEMS Handbook*; CRC Press: Florida, **2001**.
2. T. Bourouina, A. Bosseboeuf, and J. P. Grandchamp, *J. Micromech. Microeng.* 7, 186 (**1997**).
3. S. Shoji and M. Esashi, *J. Micromech. Microeng.* 4, 157 (**1994**).
4. M. T. A. Saif, B. E. Alaca, and H. Sehitoglu, *J. Microelectromech. S.* 8, 335 (**1999**).
5. E. Makino, T. Mitsuya, and T. Shibata, *Sensor Actuat a-Phys* 88, 256 (**2001**).
6. W. B. Russel, D. A. Saville, and W. R. Schowalter, *Colloidal Dispersions*, Cambridge University Press, New York (**1989**).
7. J. H. Masliyah, *Electrokinetic Transport Phenomena*, AOSTRA, Edmonton (**1994**), Vol. 12.
8. S. L. Carnie and D. Y. C. Chan, *J. Colloid. Interf. Sci.* 155, 297 (**1993**).
9. S. L. Carnie, D. Y. C. Chan, and J. Stankovich, *J. Colloid. Interf. Sci.* 165, 116 (**1994**).
10. M. Ospeck and S. Fraden, *J. Chem. Phys.* 109, 9166 (**1998**).
11. W. R. Bowen and A. O. Sharif, *Nature* 393, 663 (**1998**).
12. P. K. Das, S. Bhattacharjee, and W. Moussa, *Langmuir* 19, 4162 (**2003**).
13. B. V. Derjaguin and L. Landau, *Acta Physicochimica (USSR)* 14, 633 (**1941**).
14. E. J. Verwey and J. T. G. Overbeek, *Theory of Stability of Lyophobic Colloids*, Elsevier, Amsterdam (**1948**).
15. S. Bhattacharjee and A. Sharma, *J. Colloid. Interf. Sci.* 171, 288 (**1995**).
16. R. J. Hunter, *Foundations of Colloidal Science*, Oxford University Press, New York (**2001**), 2nd ed.

Received: 17 December 2003. Accepted: 3 January 2004.

RESEARCH ARTICLE